Journal of Magnetism and Magnetic Materials 369 (2014) 142–146

Contents lists available at ScienceDirect

Journal of Magnetism and Magnetic Materials

journal homepage: www.elsevier.com/locate/jmmm

Temperature induced ferromagnetic resonance frequency change and resonance line broadening of a Fe–Co–Hf–N film with in-plane uniaxial anisotropy – a theoretical and experimental study

K. Seemann *, K. Krüger, H. Leiste

Karlsruhe Institute of Technology KIT (Campus North), Institute for Applied Materials, Hermann-von-Helmholtz-Platz 1, 76344 Eggenstein-Leopoldshafen, Germany

ARTICLE INFO

Article history:
Received 14 May 2014
Received in revised form
4 June 2014
Available online 13 June 2014

Keywords:
Ferromagnetic film
Temperature-dependent FMR
Line broadening
Intrinsic damping

ABSTRACT

A soft ferromagnetic Fe–Co–Hf–N film was produced by reactive r.f. magnetron sputtering, in order to study its high-frequency behaviour by means of frequency domain permeability measurements up to the GHz range. It resulted in the composition $Fe_{33}Co_{43}Hf_{10}N_{14}$ and exhibits a saturation polarisation J_s of around 1.35 T. The film is consequently considered as being uniformly magnetised due to an in-plane uniaxial anisotropy of approximately $\mu_0.H_u \approx 4.5$ mT after annealing it at 400 °C in a static magnetic field for 1 h. While heating the film from room temperature to 300 °C during the high-frequency measurement procedure a marked ferromagnetic resonance peak shift (maximum of the imaginary part of the frequency-dependent permeability) from 2.35 GHz down to 1.84 GHz is conspicuous. This is in a very good agreement with the theory established by taking the "real" ferromagnetic resonance formula for ferromagnetic films into account. Simultaneously, the full width at half maximum (FWHM) Δf_{FMR} of the resonance line, which is a consequence of precession damping of the magnetic moments, clearly increases. This behaviour does not correlate with the ferromagnetic resonance value decrease, and is qualitatively discussed in terms of exchange interaction with the intrinsic spin–lattice relaxation process due to not totally supressed orbital momenta ($\langle L\rangle \neq 0$) of Fe^{2+} and Co^{2+} or the occupation change of their spectral levels within the induced uniaxial anisotropy field.

1. Introduction

The behaviour of ferromagnetic transition metal spin moments in a ferromagnetic film, which are driven by a magnetic high-frequency field to precess about their preferred direction in an external or anisotropy field, is of special interest in terms of resonance, permeability and damping behaviour. The Landau–Lifschitz–Gilbert differential equation (LLG)

$$\frac{\partial \vec{M}}{\partial t} = -\gamma \vec{M} \times \vec{H}_{eff} + \frac{\alpha}{M_s}\left(\vec{M} \times \frac{\partial \vec{M}}{\partial t}\right) \quad (1)$$

[1], although quasi-classical in nature, perfectly describes the dynamics of these ferromagnetic moments in a wide frequency range. Magnetic films, where demagnetisation effects influence the magnetic moments, need a special "anisotropic" solution of their dynamics, i.e., an anisotropic solution of the LLG [2]. For convenience, eddy-currents in a film can be neglected if it is thin enough and possesses a sufficiently high resistivity. But what about the thermal impact on its dynamics? Excellent experimental research on the temperature-dependent dynamics up to 420 K was made by [3] and [4]. The authors showed that there is a non-negligible temperature impact on the frequency behaviour.

Certain concepts like sensor applications where ferromagnetic films are exposed to changes of temperature [5] or stress [6] need a deeper insight into the temperature-dependent dynamic film properties. Therefore, the present work focuses on parameters such as damping processes, i.e., resonance line broadening and magnetisation which could vary due to the temperature impact as well as the in-plane uniaxial anisotropy change by thermal fluctuations. Due to the substrate-film arrangement thermal expansion, resulting in film stress, may also play a role which impacts the frequency behaviour via the magnetoelastic anisotropy contribution. Since the material system Fe–Co–Hf–N shows sufficient soft magnetic and acceptable magnetoelastic properties as well as excellent frequency suitability [7–9], it makes sense to utilise this material for thermal investigations. Accordingly, we also like to focus our attention on the approach of a theoretical description of the temperature dependent ferromagnetic resonance frequency (FMR) and resonance line broadening. Finally, the comparison with experimental data is carried out and discussed.

* Corresponding author. Tel.: +49 721 608 24255; fax: +49 721 608 24567.
E-mail address: klaus.seemann@kit.edu (K. Seemann).

http://dx.doi.org/10.1016/j.jmmm.2014.06.022
0304-8853/

2. Theory of the temperature dependent FMR

In order to theoretically describe the influence of temperature on the frequency behaviour of a ferromagnetic film with an in-plane uniaxial anisotropy, we need an advanced description of the ferromagnetic resonance frequency. A more precise resonance frequency formula than the frequently used Kittel resonance formula, which is valid for $\alpha \ll 1$ or equal to zero, was elaborated in [10] by solving the "anisotropic" LLG. It has the following form,

$$f_{\mathrm{FMR}} = \frac{\gamma}{2\pi(1+\alpha^2)}\mu_0\sqrt{H_{\mathrm{u}}^2 + H_{\mathrm{u}}M_{\mathrm{s}} - \frac{M_{\mathrm{s}}^2\alpha^2}{4}}, \tag{2}$$

in which $\gamma \sim 190$ GHz/T is the gyromagnetic and μ_0 the magnetic field constant. Considering the saturation magnetisation M_{s}, the general damping parameter α and the in-plane uniaxial anisotropy field H_{u} it seems likely that all these parameters possess temperature dependence. Firstly, the temperature dependence of M_{s} is well known from literature. At this point we use the saturation polarisation $J_{\mathrm{s}}(T) = \mu_0 M_{\mathrm{s}}(T)$ which must be numerically computed by using the Brillouin function $B(a)$

$$\mu_0 M_{\mathrm{s}}(T) = J_{\mathrm{s}}(T) = \mu_0 N g_{\mathrm{S}} \mu_{\mathrm{B}} S B(a)$$
$$= \mu_0 N g_{\mathrm{S}} \mu_{\mathrm{B}} S\left(\frac{2S+1}{2S}\coth\left(\frac{2S+1}{2S}a\right) - \frac{1}{2S}\coth\left(\frac{a}{2S}\right)\right). \tag{3}$$

For ferromagnetic materials the argument of $B(a)$ is

$$a = \frac{g_{\mathrm{S}}\mu_{\mathrm{B}} S \nu J_{\mathrm{s}}(T)}{k_{\mathrm{B}}T}. \tag{4}$$

In (3) and (4), N is the number of ferromagnetic ions, $g_{\mathrm{S}} \sim 2$ is the spin g-factor, μ_{B} is the Bohr magneton, S is the total spin quantum number, ν is the molecular field constant, k_{B} is the Boltzmann constant and T is the temperature.

Secondly, the temperature dependent damping parameter $\alpha(T)$ can be written in the following expression [11]

$$\alpha(T) = \frac{G}{\gamma J_{\mathrm{s}}(T)} \tag{5}$$

in which G is the Gilbert damping parameter.

The last and crucial parameter which also depends on temperature is the in-plane uniaxial anisotropy. It has to be considered separately and is substituted by an effective anisotropy field $H_{\mathrm{a}}^{\mathrm{eff}}$ in (2) which is additionally impacted by the magnetoelastic anisotropy field H_{me} through thermally induced strain and/or stress due to a ferromagnetic film-substrate configuration as well as thermal fluctuations implicitly expressed by H_{u}.

In the first step, we regard the uniaxial anisotropy in the y-direction and write the effective anisotropy in a general vector form [12]

$$\mu_0 H_a^{eff}(T) = \mu_0 H_u(T) + \mu_0 H_{me}(T)$$
$$= \mu_0\begin{pmatrix} 0 \\ H_{\mathrm{u}}(T) \\ 0 \end{pmatrix} + \mu_0\begin{pmatrix} \frac{3\lambda_s}{J_s(T)}\sigma_{\mathrm{x}}(T) \\ \frac{3\lambda_s}{J_s(T)}\sigma_{\mathrm{y}}(T) \\ 0 \end{pmatrix} \tag{6}$$

for which we calculate the absolute value by assuming isotropic stress ($\sigma_x = \sigma_y = \sigma$) due to thermally induced isotropic strain ε

$$\mu_0\left|H_{\mathrm{a}}^{\mathrm{eff}}(T)\right|$$
$$= \sqrt{(\mu_0 H_{\mathrm{u}}(T))^2 + 2\left(\frac{3\mu_0\lambda_s\sigma(T)}{J_{\mathrm{s}}(T)}\right)^2 + \mu_0 H_{\mathrm{u}}(T)\frac{6\mu_0\lambda_s\sigma(T)}{J_s(T)}}. \tag{7}$$

The magnitude λ_{s} represents the saturation magnetostriction. To simplify matters λ_{s} is considered as a constant. In order to obtain the relation between stress and strain, the general Hook's law

$$\sigma = \frac{E_{\mathrm{s}}}{1-\nu_{\mathrm{s}}}\varepsilon, \tag{8}$$

with the Young's modulus E_{s} of the substrate and the Poisson's number ν_{s} was taken into account. In case of a single crystalline substrate (Si (100)) the expression $E_{\mathrm{s}}/1-\nu_{\mathrm{s}}$ is substituted by the biaxial modulus $M = 180.3 \times 10^9$ N/m^2 [13]. The common strain at the substrate surface, $\varepsilon = t_{\mathrm{s}}/2r$, can be formulated by assuming that the neutral axis is located in the centre of the substrate with thickness t_{s} much higher than the film thickness. Due to different thermal expansion parameters of the film-substrate arrangement the whole structure is bended to a radius r if the temperature T is varied. By taking the Stoney equation into account

$$\varepsilon_{\mathrm{mech}} = \frac{1}{6}\frac{t_{\mathrm{s}}^2}{t_{\mathrm{f}}r}, \tag{9}$$

which now considers the film thickness t_{f}, the mechanical strain can be put on the same level with the thermal strain

$$\varepsilon_{\mathrm{th}} = (\alpha_{\mathrm{f}} - \alpha_{\mathrm{s}})(T_1 - T) = \Delta\alpha_{\mathrm{fs}}\Delta T \tag{10}$$

for which $T_1 < T$. α_{f} and α_{s} are the thermal expansion coefficients of the film and the substrate, respectively. As a result the radius calculates to

$$r = \frac{1}{6}\frac{1}{\Delta\alpha_{\mathrm{fs}}\Delta T}\frac{t_{\mathrm{s}}^2}{t_{\mathrm{f}}} \tag{11}$$

which is put into Eq. (8) we need for the magnetoelastic anisotropy contribution, $3\lambda_{\mathrm{s}}\sigma(T)/J_{\mathrm{s}}(T)$, in (6).

Finally, one has to be aware of the "intrinsic" temperature dependence of H_{u}. For its description one can correlate the anisotropy coefficient K_{u} with the temperature dependent saturation magnetisation. In order to arrange it, we manage with the "power law" according to [14] and [15]

$$K_{\mathrm{u}}(T) = K_{\mathrm{u}}(0)\left(\frac{J_{\mathrm{s}}(T)}{J_{\mathrm{s}}(0)}\right)^{\frac{n(n+1)}{2}} \tag{12}$$

which we assume as a more simple description for the temperature dependent in-plane uniaxial anisotropy in a temperature range between RT and 300 °C (573 K)

$$\mu_0 H_{\mathrm{u}}(T) = \mu_0\frac{2K_{\mathrm{u}}(T)}{J_{\mathrm{s}}(T)} = \mu_0\frac{2K_{\mathrm{u}}(0)}{J_{\mathrm{s}}(T)}\left(\frac{J_{\mathrm{s}}(T)}{J_{\mathrm{s}}(0)}\right)^m \tag{13}$$

Here, $K_{\mathrm{u}}(0)$ is the uniaxial anisotropy coefficient at $T \sim 0$, and m is an integer.

All temperature dependent parameters are now established and can be applied in Eq. (2) which results in a comprising formulation of the temperature dependent ferromagnetic resonance frequency.

3. Experimental

A soft ferromagnetic Fe–Co–Hf–N nanocomposite film was deposited onto a Si (100) substrate with 1 µm silicon oxide (5 mm × 5 mm × 0.375 mm) by reactive r.f. magnetron sputtering in an Ar/N_2 atmosphere at a constant pressure of 0.5 Pa and at a sputtering power of 250 W. The argon/nitrogen gas flow fraction was kept constant at 97 sccm/3 sccm which resulted in the film composition $Fe_{33}Co_{43}Hf_{10}N_{14}$, determined by electron probe microanalysis (EPMA). The film thickness was approximately 190 nm. For deposition, a 6 in. target (target composition: $Fe_{37}Co_{46}Hf_{17}$) was used in a Leybold Heraeus Z550 sputtering device. During an annealing process in a static magnetic field a uniaxial anisotropy in the film plane was induced. The polarisation $J(\mu_0 H_{\mathrm{ext}})$ loop of the in-plane easy and hard direction of the magnetic polarisation was measured by means of a vibrating sample magnetometer (VSM), in

order to measure the initial saturation polarisation J_s as well as the initial uniaxial anisotropy field $\mu_0 H_u$ at room temperature (RT).

An improved and heatable strip-line permeameter (RT to 300 °C), connected to an Agilent E5071C ENA network analyser, was developed to carry out the in-plane frequency characterisation with the high-frequency field perpendicular to the easy direction of polarisation, i.e., the in-plane uniaxial anisotropy. In Fig. 1, the set-up is illustrated in detail. The frequency-dependent permeability was determined after evaluating the one port S_{11}-parameter from 100 MHz up to 5 GHz [16]. The resistivity of the film amounted to around 1.2 μΩm which was measured by means of a 4-point probe. Due to the fairly high resistivity and in consideration of the fact that the film is thin enough, eddy currents can be neglected.

4. Experimental results and verification with the theory

After measuring the static polarisation a saturation polarisation J_s of 1.35 T and a distinct in-plane uniaxial anisotropy of around 4.5 mT could be observed (Fig. 2). As a result, the film can then be considered as being uniformly magnetised in one direction which tends the magnetic moments to process in a uniform manner. In this case and from experience, the validity of LLG for describing the FMR experiment is given as shown in Fig. 3, in which the real- and imaginary part of the frequency-dependent permeability at room temperature reflect a good correspondence to the measured data. The resonance frequency of the spectrum amounts to 2.35 GHz with an initial permeability $\mu_r(f=100\ \text{MHz})$ of around 280. The damping parameter promises $\alpha \sim 0.005$. In Fig. 4, the frequency-dependent permeability is exhibited for three different temperatures. It can be

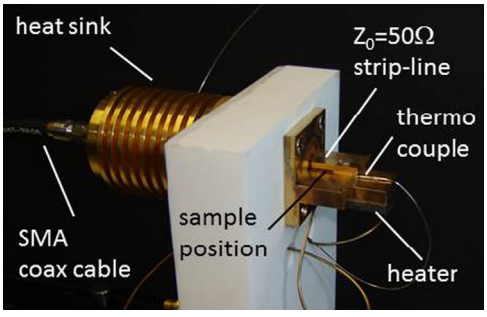

Fig. 1. Heatable strip-line permeameter for high-frequency measurements up to 5 GHz and temperatures from room temperature to 300 °C (573 K).

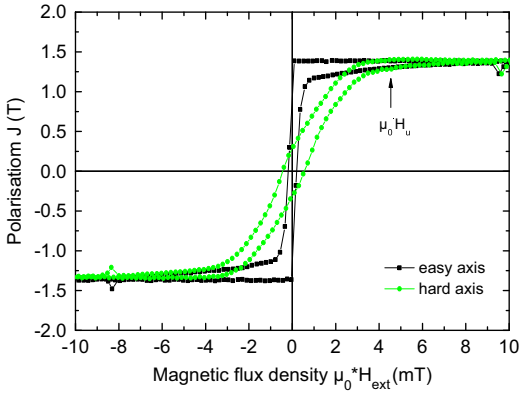

Fig. 2. Hard and easy axis polarisation curves of a $Fe_{33}Co_{43}Hf_{10}N_{14}$ film annealed at 400 °C (673 K) for 1 h in a static magnetic field. The thickness of the film is approximately 190 nm.

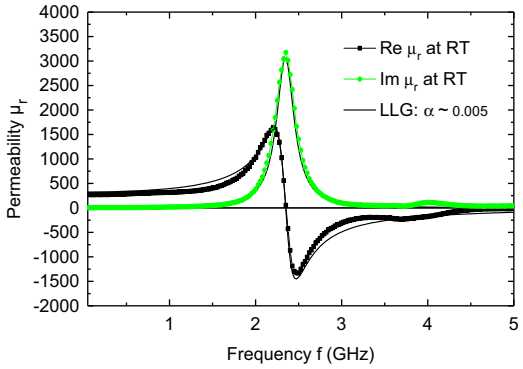

Fig. 3. Real and imaginary part of the frequency-dependent permeability of a $Fe_{33}Co_{43}Hf_{10}N_{14}$ film with a thickness of approximately 190 nm. The film was measured at room temperature (RT). The damping parameter α(RT) for the LLG fit amounts to 0.005.

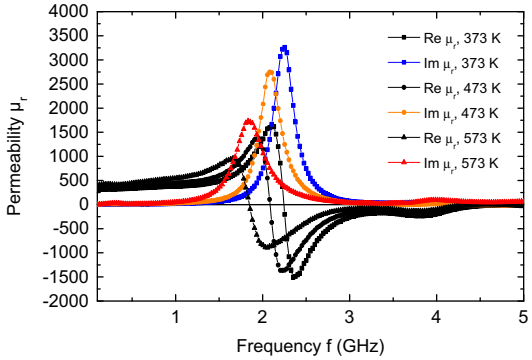

Fig. 4. Real and imaginary parts of the frequency-dependent permeability of a $Fe_{33}Co_{43}Hf_{10}N_{14}$ film with a thickness of approximately 190 nm measured at the temperatures 373, 473 and 573 K.

observed that, e.g., the maximum of the imaginary part of the resonance curve decreases and is located at lower frequencies with a temperature up to 300 °C. The second very small peak which appears at around 4 GHz is often attributed to strip domains [17]. But due to the fact that the film is annealed in a magnetic field stripe domains can be excluded. Consequently, the second peak may reveal slight uncertainties in the network analyser calibration. In Fig. 5, the FMR is plotted versus the temperature in a closer measure, and it can be seen that it gradually decreases in a non-linear way. By comparing the experimental data to the theory, which is finally represented by formula (2) including Eqs. (3)–(13), the FMR values match the theory in the realised temperature range. The dashed part of the theoretic curve at higher temperatures (Fig. 5) is predominantly affected by a sudden increase of the uniaxial anisotropy, and herewith the rise in FMR, due to thermal stress until FMR becomes zero caused by magnetic phase transition at the Curie temperature T_c. It can be estimated to be around 1080 K which is very close to the Curie temperature of Fe–Co in the composition shown above. At lower temperatures the FMR does not really change because the saturation polarisation versus temperature remains nearly constant.

Having a closer look to the full width at half maximum (FWHM) of the imaginary part of the spectra one is able to observe a steep slope approximately between 450 and 500 K before a maximum seems to appear at around 540 K (Fig. 6). At higher temperatures the FWHM seems to decline which results in lower damping of the precessing magnetic moments again. This resonance line broadening characteristic does not correlate with the ferromagnetic

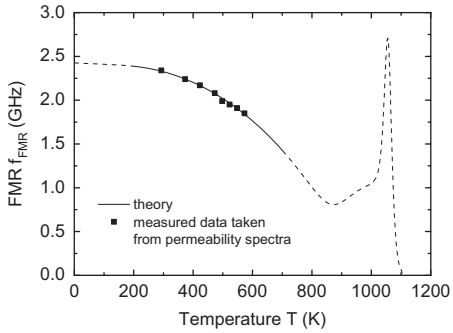

Fig. 5. Ferromagnetic resonance frequency dependent on temperature. The solid/dashed curve shows the theoretical model. Essential parameters for the theoretic computation are as follows: $N=4\times10^{28}$ 1/m^3, $S=3/2$, $\nu=620$, $G=1.33\times10^9$ 1/s, $\lambda_s=60\times10^{-6}$, $\alpha_f=11.3\times10^{-6}$ 1/K, $\alpha_s=2.7\times10^{-6}$ 1/K, $K_u(0)=2.55\times10^3$ J/m^3, $m=3$.

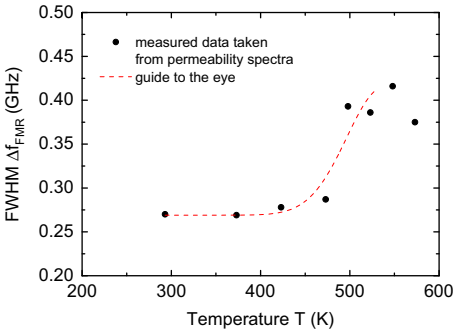

Fig. 6. Full width at half maximum of the ferromagnetic resonance peak dependent on the temperature. The solid line fits the data as a guide to the eye.

resonance frequency increase which indicates another effect to be discussed in the following section.

5. Discussion and conclusion

By using the complete formula for the ferromagnetic resonance frequency with respect to damping and substituting the parameters by the temperature-dependent parameters it is possible to describe f_{FMR} in a comprising way. While the experimental resonance data match the theoretic curve well, Δf_{FMR} shows a totally different and uncorrelated behaviour. This behaviour was observed in rare earth ion garnets [18] where damping occurs via the fast relaxing rare earth ion which is highly coupled to the lattice due to a strong L–S coupling.

Since Fe^{2+} und Co^{2+} belong to fast relaxing ions with orbital momenta L which are not totally quenched, it is apparent that one assumes the origin of the observed resonance line broadening in intrinsic spin–lattice relaxation effects due to direct energy dissipation from the spin system to the lattice. This process results in a homogeneous line broadening increase. Due to the fact that there is one observed maximum in Δf_{FMR} by trend it can be also assumed that the actual broadening mechanism can be found in the temperature dependent exchange interaction between the processing ion spins which are arranged in an anisotropic short-range order and which are coupled to lattice vibrations (phonons) via spin–orbit coupling. By increasing the temperature the exchange interaction, the saturation polarisation and anisotropy between the magnetic elements is precociously weakened. Using the theoretical assumptions made here one attributes the condition $\tau\omega_{ex}\sim1$ to the maximum of $2\pi\Delta f_{FMR}$ [18]. With the exchange frequency $\omega_{ex}=2\pi\nu(\gamma_{Fe}J_{Co}+\gamma_{Co}J_{Fe})\sim4.7\times10^{14}$ 1/s, the relaxation time τ results in around 2×10^{-15}s which is allocated to the ion with "fast relaxation", but unfortunately does not reflect the experimentally determined FWHM. As a consequence, a "slow relaxation" process with time τ is more obvious where the energy exchange between Fe^{2+} and Co^{2+} and the energy dissipation via spin–lattice relaxation dependent on temperature through both elements still occurs. But at this point we cannot define the ferromagnetic transition element with the dominant relaxation behaviour. Anyway, since there is a maximum in $\Delta f_{FMR}(T)$, at which the condition $\tau2\pi f_{FMR}\sim1$ is assumed for "slow relaxation" [19], a mean resonance line width is determined by spectral energy transitions between magnetic energy levels where the induced uniaxial anisotropy field defines their distance because the magneto-crystalline anisotropy is at a minimum. If the temperature is increased the common spectral transition (uniaxial anisotropy) is perturbed and damping occurs more and more via dissipation of the energy by interaction with phonons. By these conditions the observed maximum in Δf_{FMR} let us calculate the relaxation time to be $\tau\sim8.2\times10^{-11}$ s which is usually attributed to the ion with the higher damping property. This is closer to the mean relaxation time ($\sim3.8\times10^{-10}$ s) attained from $2\pi\Delta f_{FMR}$ at around 540 K. For higher temperatures now, the ion with higher damping is gradually decoupled from the lower damped ion by weakening the mean uniaxial anisotropy. That is, it cannot follow the precession of the lower-damped ion which individually processes and still interacts with the lattice, while f_{FMR} also decreases due to the decreasing anisotropy. As a result, $2\pi\Delta f_{FMR}$ begins to decrease in trend which is indicated for a higher temperature value (Fig. 6).

The explanations of the scientific work described above reveal achievements which are useful for applications in magnetic sensors for monitoring, e.g., temperature induced mechanical stress. But disadvantages due to thermal impact may also be present in microelectronic applications such as MRAMs, where magnetic spins enable information storage. Here, the access time may be influenced in a negative way. Utilising ferromagnetic films in micro-inductors precession damping of magnetic moments can lead to higher losses in a certain frequency range in which more energy is absorbed.

Acknowledgement

This work was partially carried out with the support of the Karlsruhe Nano Micro Facility (KNMF, www.knmf.kit.edu), a Helmholtz research infrastructure at Karlsruhe Institute of Technology (KIT, www.kit.edu).

References

[1] T.L. Gilbert, IEEE Trans. Magn. 40 (2004) 3443.
[2] K. Seemann, H. Leiste, V. Bekker, J. Magn. Magn. Mater. 278 (2004) 200.
[3] N.N. Phuoc, G. Chai, C.K. Ong, J. Appl. Phys. 112 (2012) 083925.
[4] N.N. Phuoc, C.K. Ong, Adv. Mater. 25 (2013) 980.
[5] A. Ludwig, M. Tewes, S. Glasmachers, M. Löhndorf, E. Quandt, J. Magn. Magn. Mater. 242–245 (2002) 1126.
[6] C. Thede, S. Chemnitz, I. Teliban, Ch. Bechtold, Ch. Klever, M. Stüber, E. Quandt, Sens. Actuators A: Phys. 178 (2012) 104.
[7] K. Seemann, H. Leiste, Ch. Klever, J. Magn. Magn. Mater. 321 (2009) 3149.
[8] K. Seemann, H. Leiste, Ch. Klever, J. Magn. Magn. Mater. 322 (2010) 2979.
[9] N.N. Phuoc, L.T. Hung, C.K. Ong, J. Alloys Compd. 509 (2011) 4010.
[10] K. Seemann, H. Leiste, K. Krüger, J. Magn. Magn. Mater. 345 (2013) 36.
[11] K. Lenz, H. Wende, W. Kuch, K. Baberschke, Phys. Rev. B 96 (2006) 144424.
[12] K. Krüger, K. Seemann, H. Leiste, M. Stüber, S. Ulrich, J. Magn. Magn. Mater. 343 (2013) 42.

[13] G.C.A.M. Janssen, M.M. Abdalla, F. van Keulen, B.R. Pujada, B. van Venrooy, Thin Solid Films 517 (2009) 1858.
[14] C. Zener, Phys. Rev. 96 (1954) 1335.
[15] J.B. Staunton, L. Szunyogh, A. Buruzs, B.L. Gyorffy, S. Ostanin, L. Udvardi, Phys. Rev. B 74 (2006) 144411.
[16] V. Bekker, K. Seemann, H. Leiste, J. Magn. Magn. Mater. 270 (2004) 327.
[17] N.N. Phuoc, C.K. Ong, J. Appl. Phys. 114 (2013) 023901.
[18] C. Kittel, J. Appl. Phys. 31 (5) (1960) 11S–13S.
[19] S. Krupicka, Physik der Ferrite und der verwandten magnetischen Oxide, Friedr. Vieweg and Sohn Braunschweig (1973) 533.